

Phase diagram of a growing succinonitrile crystal in supercooling-anisotropy phase space

H. Honjo and S. Ohta

College of General Education, Kyushu University, Ropponmatsu, Fukuoka 810, Japan

M. Matsushita

Department of Physics, Faculty of Science and Engineering, Chuo University, Kasuga, Bunkyo-ku, Tokyo, 112, Japan

(Received 24 April 1987; revised manuscript received 10 August 1987)

The phase diagram of growing crystal patterns for succinonitrile is obtained experimentally in a supercooling-anisotropy phase space. The anisotropy of the crystal growth is changed by roughening the upper surface of the bottom plate of the thin crystal-growth cell. Various growing modes are observed, and the relation between regular dendritic and random diffusion-limited-aggregation-like crystals is discussed.

Recently, many investigations of the pattern formation in the diffusion field have emerged and the understanding of its mechanism has been gradually made clear. One of the most interesting examples is diffusion-limited aggregation¹ (DLA), which is a simple yet realistic model idealizing pattern formation in the Laplace field, such as electrostatic potential, pressure, and concentration fields.² It produces isotropically ramified fractal patterns. The growing mechanism of a DLA cluster is summarized as follows: The majority of random walkers launched far away from the cluster are captured by protruding main branches and produce the backbone of the cluster, while the residual ones, which happen to enter into "fjords" to some extent, complete the self-similar structure.^{3,4}

On the other hand, it is well known that the diffusion field with some boundary condition such as anisotropy or surface tension brings about regular patterns. A typical example is dendritic crystal growth, which has been investigated as the problem of interfacial instability in a nonlinear system.⁵ A few models in the dendritic crystal growth have been proposed so far. In the geometric model,⁶ the interfacial dynamics is assumed to be determined only by the local curvature of interface. The simulation results of the model show that there exists a critical value of the anisotropy strength distinguishing tip-splitting growth mode from tip-oscillating mode. This model does not seem to correspond to real crystal growth. A new analytic approach, the solvability condition,^{6,7} has been introduced. It shows that while without any microscopic dynamics, such as surface tension, there exists an infinite family of solutions for steady-state patterns (Ivantsov solution⁸), which breaks down to a discrete set when the microscopic parameter is included. This approach is also used to obtain steady-state patterns in a fully nonlocal model⁹ and a boundary-layer model.¹⁰ The boundary layer model is a nonlocal one and is still investigated actively. The successive side branches are generated in this model by selective amplification of noise near the tip,¹¹ instead of deterministic dynamics such as tip oscillation. Here, one should pay attention to the result that the stable tip needs nonzero anisotropy.

The relation between DLA and dendrite has recently been discussed with both experiments and simulations.

The crucial point in understanding it is the degree of anisotropy of the system. The experimental phase diagram of viscous fingering has been obtained by varying the background anisotropy of a Hele-Shaw cell and the injected pressure of a lower-viscosity fluid.¹² In this experiment, faceted, tip-splitting, needlelike, and dendritic patterns have been observed. Moreover, the simulation of viscous fingering by using random walkers exhibits tip-oscillating, tip-splitting, and DLA-like patterns according to the variation of the nondimensional parameter B , which corresponds to the strength of the unidirectional anisotropy.¹³

The viscous finger itself is essentially isotropic and therefore the anisotropy should come from the external boundary condition. On the contrary, the growing crystal intrinsically contains the strong crystalline anisotropy, and it is usually observed as a regular pattern dendrite (here we restrict ourselves to the growth region limited by the diffusion in liquid). Recently, we reported DLA-like crystal growth from the aqueous solution of NH_4Cl in the Hele-Shaw-like cell, one of the glass-plate surfaces of which is roughened to weaken the degree of the crystal-growth anisotropy.¹⁴ Its fractal dimension is 1.671 ± 0.002 and is in very good agreement with the theoretical prediction.⁴

In this paper we investigate the importance of the anisotropy of growing crystal and show the phase diagram of succinonitrile in a supercooling-anisotropy phase space. The growing patterns exhibit various growing behaviors such as tip-splitting, tip-oscillating, and tip-stable modes.

In Fig. 1 we show the experimental setup. The crystal-growth cell is made quasi two dimensionally and the thickness of the spacer d is $14 \mu\text{m}$. The thin bottom glass (the thickness is approximately 0.3 mm) is scratched randomly [the characteristic length of the roughness is l (μm)] and attached to a sapphire glass. The roughness l means that the two-dimensional (horizontal) roughness is of order l . The value of l is determined from the image analysis (two-dimensional Fourier spectrum analysis) of the pictures of roughened glass. It is expected that the glass is roughened vertically by the same order because the glass is scratched by abrasives. This glass is pasted on a current-conductive glass and the temperature of this sys-

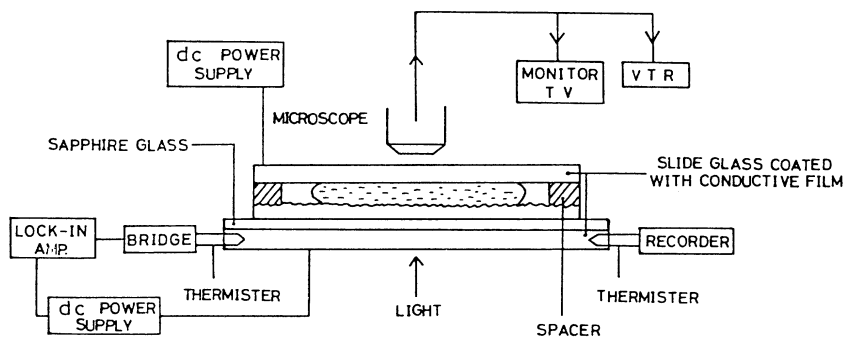


FIG. 1. The experimental setup. Succinonitrile is sealed in the quasi-two-dimensional cell whose bottom glass is roughened randomly. The pictures are taken using a video tape recorder.

tem is controlled by the current through the bridge circuit. The accuracy of the controlled temperature is $\pm 0.025^\circ\text{C}$. Succinonitrile is sealed in this thin cell. The pictures of growing crystals are taken using a video tape recorder through a microscope and a TV camera, and then processed by the image analysis technique. Succinonitrile is a transparent plastic crystal at room temperature and has fourfold symmetry.¹⁵ A crystalline anisotropy is originally determined microscopically as the strength of bonding between atoms and its value is constant. However, as long as we pay attention to the macroscopic growing pattern and its growth direction under the perturbations, we can introduce α as the *growth directional anisotropy* of the pattern.

Let us define α by $\alpha \equiv d/l$ considering only the geometry of the cell as introduced by Ben-Jacob *et al.*¹² in the experiment of viscous fingering with background anisotropy. This definition results from the estimation as follows. In the case of $l \ll l_c$, l_c is the characteristic length of the crystal such as the tip radius of curvature; α is much stronger because very small-sized perturbations are averaged out to yield no influence to the growth direction. The larger l makes influence to the crystal tip stronger, and when $l \sim l_c$, the tip is influenced very strongly by the roughness. Furthermore, d enhances the above effect. As we will show later, the growth behavior depends on supercooling, that is, l_c . We change the roughness by three cases $l = 34, 16,$ and $10 \mu\text{m}$. These values are averaged ones and each variance of the roughness is about $\pm 1/2$.

The thermal conductivities of liquid succinonitrile at melting point and the roughened glass are $k_{\text{su}} = 5.32 \times 10^{-4} \text{ cal/cm s K}$ and $k_{\text{gl}} = 1.44 \times 10^{-3} \text{ cal/cm s K}$ ($\approx 2.7k_{\text{su}}$), respectively. This means that our system of melt growth is three dimensional in thermal diffusion. The crystal tends to grow toward the protrusions on the surface of the randomly roughened glass, which give random perturbations to the crystal tip. The succinonitrile is first crystallized and then melted until only one small seed is left. It takes some time for the system temperature to reach the required value. Since the initial instability from the seed crystal is inevitably truncated due to the limited range of our microscope vision, we look at the growing tip, and not a global pattern. We vary the supercooling temperature $\Delta\theta (= T_M - T_\infty)$ at any fixed α to make a phase diagram. Here T_M is the melting point of succinonitrile

($\approx 54.5^\circ\text{C}$) and T_∞ is the temperature of the system.

Let us survey the typical growing patterns according to $\Delta\theta$ in the case of $\alpha = 0.875$. For smaller $\Delta\theta$ (0.44°C), the growing mode is tip splitting [Fig. 2(a)]. We also show a schematic picture in Fig. 2(b). The tip curvature and velocity oscillate, and the growth direction also oscillates. The preferred growth direction is $\langle 100 \rangle$. One can see two sharp protrusions A and B in Figs. 2(a) and 2(b). A is in fresher liquid than B and grows as the tip. The position of B grows slowly to another direction as a side branch. This phenomenon is observed as tip splitting. Because the growth direction of the tip A is not originally preferred, the tip velocity is decelerated and the tip curvature becomes smaller, and the growth direction recovers to $\langle 100 \rangle$. On that occasion, there remains a protrusion C (Fig. 2), which grows as a side branch. Consequently, this side branch C is asymmetric with the tip-split side branch B , and does not develop well because the supercooling here is reduced by the heat diffused from the tip. The global pattern is observed as follows: The tip-split side branches are well developed, while those on another side do not grow so well, and side branches of both sides are asymmetric. We call this growth mode the asym-

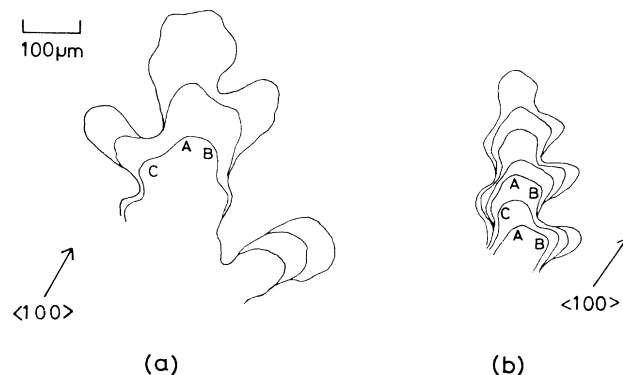


FIG. 2. (a) Growing patterns overlapped in arbitrary time interval in the case of small $\Delta\theta$ ($= 0.44^\circ\text{C}$). A is the tip, B grows as a well-developed side branch, and C grows as a less-developed one. The growing behavior is the asymmetric tip-splitting (ATS) mode. (b) Overlapped schematic picture of Fig. 2(a). A , B , and C are the same with Fig. 2(a).

metric tip-splitting (ATS) mode.

When $\Delta\theta$ is larger (1.99°C), the growing mode is still tip splitting (Fig. 3). The growth mechanism is the same as seen in Fig. 2. However, because of the larger supercooling the two sharp protrusions can grow together as tips. After the tip splitting, each tip grows with ATS mode because the distance between the two tips is close and local supercooling around there is smaller. After the tips grow far apart from each other, they repeat the tip splitting. This growth mode is characterized as the simultaneous growth of the two split tips. Let us call this mode symmetric tip-splitting (STS) mode.

When $\Delta\theta$ is increased more (2.44°C), the tip splitting cannot occur any more (Fig. 4). The tip radius is smaller, and becomes more stable than former cases. The averaged growth direction is $\langle 100 \rangle$. The disturbance from the rough surface of the cell brings about the tip oscillation, which causes asymmetric side branching. Although the asymmetry of side branches is not clear in this figure, we can identify it from the tip-oscillating growth in NH_4Cl solution.¹⁶ We call this mode the tip-oscillating (TO) mode.

When $\Delta\theta$ is much larger, the tip is very stable and the roughness causes much less influence to the tip. The tip may grow in a stationary manner without oscillation, and a usual dendrite in free space may be observed. However, this decision is difficult because the tip grows too fast. The stable tip forms a parabolic one,^{15,16} then we call this mode the stable parabolic-tip (SPT) mode.

In Fig. 5, we show the phase diagram of growing patterns for three values of the growth directional anisotropy α . With the increase of supercooling (or anisotropy) at the fixed anisotropy (or supercooling), the pattern changes from ATS to STS and then to TO. The coexisting characteristic in these modes is tip-oscillation behavior. For smaller anisotropy the tip-splitting modes are added, and for larger anisotropy the tip-oscillation is dominant.

First, let us estimate the order of the characteristic length of our pattern l_c . We consider the pattern in TO mode (Fig. 4). The averaged velocity is $v \approx 500 \mu\text{m/s}$, the diffusion constant $D = 1.16 \times 10^{-3} \text{ cm}^2/\text{s}$. Hence, the

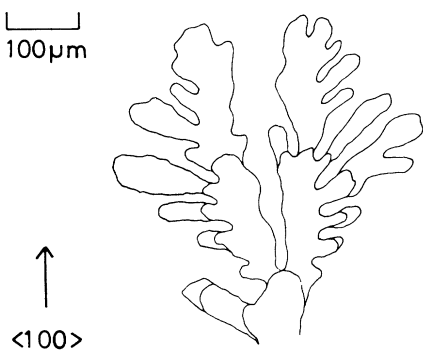


FIG. 3. Arbitrarily overlapped growing patterns in the case of large $\Delta\theta$ ($=1.99^\circ\text{C}$). The characteristic length is smaller than that in the case of Fig. 2(a) and the growing behavior is the symmetric tip-splitting (STS) mode.

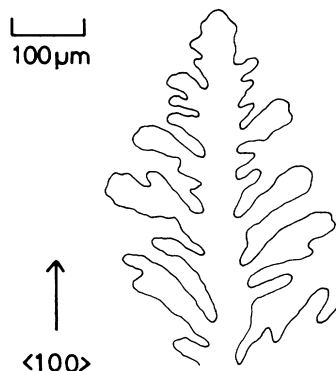


FIG. 4. The case of very large $\Delta\theta$ ($=2.44^\circ\text{C}$). The tip grows with oscillation and tip splitting cannot occur. The growing behavior is the TO mode.

diffusion length is $l_d \equiv 2D/v = 460 \mu\text{m}$. The surface tension is $\gamma = 2.14 \times 10^{-7} \text{ cal/cm}^2$, the latent heat $L = 885.1 \text{ cal/mol}$, the specific heat $c_p = 38.25 \text{ cal/mol}\cdot\text{K}$, and the melting point $T_M = 327.65 \text{ K}$, so the capillary length is $d_0 \equiv \gamma T_M c_p / L^2 = 27 \text{ \AA}$. From the Langer-Müller-Krumbhaar (LMK) theory,¹⁷ the characteristic length without roughness $l_{c0} = \rho = (l_d d_0 / \sigma^*)^{1/2} \approx 7 \mu\text{m}$. Here ρ is the tip radius of curvature and $\sigma^* = 0.025$ in three dimensions. From Fig. 4 $\rho \sim 7 \mu\text{m}$, which agrees with the above result. Strictly speaking, the tip in the LMK theory is stable, while the tip in Fig. 4 is oscillating. Nevertheless, we can roughly estimate l_c from the LMK theory. From the recent analysis considering the crystalline anisotropy of the needle crystal in a fully nonlocal model, σ^*

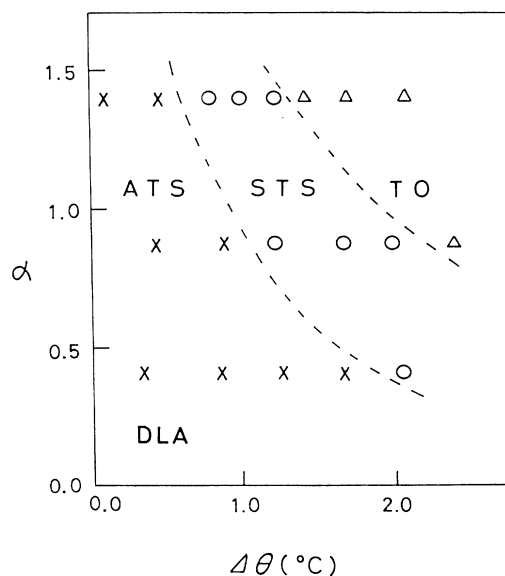


FIG. 5. Phase diagram of growing patterns in supercooling-anisotropy phase space. α is the anisotropy defined from the geometry of the cell. The tip-splitting and tip-oscillating modes are divided by the condition $\rho \sim l$. The DLA mode exists in lower α and $\Delta\theta$. A usual dendrite (TS mode) exists above the TO mode.

is rewritten as $\sigma_0 \alpha_d^{7/4}$ in two dimensions.¹⁸ Here σ_0 is of order unity and α_d is the degree of the anisotropy in capillary length (surface tension).

From the geometry of the cell we have defined α as d/l . This definition corresponds to that of Ben-Jacob *et al.*¹² and neglects the effect of l_c on α . On the other hand, the nondimensional parameter B of the simulation by Liang¹³ is defined as L_{VF}^2/W_{VF}^2 . Here L_{VF} is the characteristic length of viscous fingering and W_{VF} is the width of Hele-Shaw cell. B represents the influence of the wall on the finger width, i.e., the effective one-dimensional anisotropy. In our system, a larger l_c (smaller $\Delta\theta$) tends to make the tip more unstable (tip splitting). On the other hand, we can phenomenologically recognize that the tip splitting occurs because of weaker anisotropy. Therefore, we can suppose the real growth directional anisotropy experienced by the tip as $\tilde{\alpha}$, and it is considered a decreasing function of l_c . l_c is larger than l_{c0} because the roughness weakens $\tilde{\alpha}$. Couder, Gerard, and Rabaud¹⁹ showed experimentally that the width of a viscous finger whose tip has a bubble, which increases the anisotropy, is smaller than the one without a bubble. Furthermore, Hong and Langer²⁰ showed analytically that the effect of bubble is logarithmic to the finger width. The above discussion about the relation between $\tilde{\alpha}$ and l_c qualitatively explains their results. Moreover, $\tilde{\alpha}$ is an increasing function of the degree of the crystalline anisotropy ϵ , d/l , and k_{su}/k_{gl} . Here, the strength of thermal perturbations in our system is k_{gl}/k_{su} , which leads to the above effect on $\tilde{\alpha}$. Therefore, the variations of growing behaviors in our system can be recognized as the results of the competition between the destabilizing factor l_c and the stabilizing factors ϵ , d/l , and k_{su}/k_{gl} (Fig. 5).

There seems to exist a critical value of characteristic length l_c^* , which separates the tip-splitting mode and the tip-oscillating mode when l is constant. From Figs. 3 and 5, l_c^* exists in the vicinity of the supercooling region of Fig. 3. When the symmetric tip splitting occurs in Fig. 3 the tip radius of curvature ρ^* is about $16 \mu\text{m}$, then $\rho^* = l_c^* \sim l$ ($16 \mu\text{m}$). This leads to the result that if l_c is smaller than the spatial scale of macroscopic thermal fluctuations (l), the crystal tip grows to the thermally favorable direction with oscillation rather than with tip splitting. The transition from one growing mode to another seems to be continuous in our system. This results from the variance of roughness. If a subtle experiment without the variance of roughness is devised, the transition between growing modes may be discontinuous.

A DLA growth takes place through repeating the tip splitting irregularly, and this phenomenon corresponds to the ATS and STS modes. The STS mode clearly shows the crystalline anisotropy $\langle 100 \rangle$ direction because $\tilde{\alpha}$ is larger. We conjecture that there exists the DLA mode in the region where $\tilde{\alpha}$ is very small, i.e., α is small and l_c is large in the ATS mode (Fig. 5). A pattern with nonzero but small anisotropy in DLA simulations yields the isotropic DLA mode until some cluster size.²¹ Furthermore, recent analysis has elucidated the fractal (self-affine) structure of anisotropic clusters.²² The related discussion may be possible for the ATS and STS modes in the crystal growth and we will continue experimental investigations on the subjects.

In conclusion, we have shown that even in crystal growth, various growth modes are seen experimentally by varying not only supercooling but growth directional anisotropy.

¹T. A. Witten and L. M. Sander, Phys. Rev. Lett. **47**, 1400 (1981); Phys. Rev. B **27**, 5686 (1981).

²See, e.g., *On Growth and Form*, edited by H. E. Stanley and N. Ostrowsky (Martinus Nijhoff, the Hague, 1985).

³M. Matsushita, K. Honda, H. Toyoki, Y. Hayakawa, and H. Kondo, J. Phys. Soc. Jpn. **55**, 2618 (1986).

⁴K. Honda, H. Toyoki, and H. Matsushita, J. Phys. Soc. Jpn. **55**, 707 (1986).

⁵J. S. Langer, Rev. Mod. Phys. **52**, 1 (1980).

⁶R. Brower, D. Kessler, J. Koplik, and H. Levine, Phys. Rev. Lett. **51**, 1111 (1983); Phys. Rev. A **29**, 1335 (1984); D. Kessler, J. Koplik, and H. Levine, *ibid.* **30**, 3161 (1984); **31**, 1712 (1985).

⁷J. S. Langer, Phys. Rev. A **33**, 435 (1986); B. Caroli, C. Caroli, B. Roulet, and J. S. Langer, *ibid.* **33**, 442 (1986).

⁸G. P. Ivantsov, Dokl. Akad. Nauk. SSSR **58**, 567 (1947); G. Horvay and J. W. Cahn, Acta. Metall. **9**, 695 (1961).

⁹D. Kessler, J. Koplik, and H. Levine, Phys. Rev. A **33**, 3352 (1986).

¹⁰E. Ben-Jacob, N. Goldenfeld, J. S. Langer, and G. Schön, Phys. Rev. A **29**, 330 (1984); E. Ben-Jacob, N. Goldenfeld, B. G. Kotliar, and J. S. Langer, Phys. Rev. Lett. **53**, 2110 (1984).

¹¹R. Pieters and J. S. Langer, Phys. Rev. Lett. **56**, 1948 (1986).

¹²E. Ben-Jacob, R. Godbey, N. Goldenfeld, J. Koplik, H. Levine, T. Mueller, and M. Sander, Phys. Rev. Lett. **55**, 1315 (1985).

¹³S. Liang, Phys. Rev. A **33**, 2663 (1986).

¹⁴H. Honjo, S. Ohta, and M. Matsushita, J. Phys. Soc. Jpn. **55**, 2487 (1986).

¹⁵M. E. Glicksman, R. J. Schaefer, and J. D. Ayers, Metall. Trans. **7A**, 1747 (1976). We have referred to this reference about the physical constants of succinonitrile.

¹⁶H. Honjo, S. Ohta, and Y. Sawada, Phys. Rev. Lett. **55**, 841 (1985).

¹⁷J. S. Langer and H. Müller-Krumbhaar, Acta Metall. **26**, 1681 (1978); **26**, 1689 (1978); **26**, 1697 (1978).

¹⁸A. Barbieri, D. C. Hong, and J. S. Langer, Phys. Rev. A **35**, 1802 (1987). See also, J. S. Langer and D. C. Hong, *ibid.* **34**, 1462 (1986).

¹⁹Y. Couder, N. Gérard, and M. Rabaud, Phys. Rev. A **34**, 5175 (1986).

²⁰D. C. Hong and J. S. Langer (unpublished).

²¹P. Meakin, Phys. Rev. A **33**, 3371 (1986).

²²F. Family and H. G. E. Hentschel, Faraday Discuss. Chem. Soc. (to be published).